Solar RRL

WILEY VCH

Solar RRL

RESEARCH ARTICLE OPEN ACCESS

Results of an International Comparison of Indoor Photovoltaic Measurements Among Seven Metrological Institutes

Afsaneh Eghbali[1] | Petri Kärhä[1] | Erkki Ikonen[1,2] | Ingo Kröger[3] | Yean-San Long[4] | Min-An Tsai[4] | Karsten Bothe[5] | David Hinken[5] | Özcan Bazkir[6] | Jimmy Dubard[7] | Pierre Betis[7] | George Koutsourakis[8] | James Blakesley[8] | Daniel E. Parsons[8] | Stefan Winter[3]

[1]Metrology Research Institute, Aalto University, Espoo, Finland | [2]VTT MIKES, Espoo, Finland | [3]Physikalisch-Technische Bundesanstalt, Braunschweig, Germany | [4]Centre for Measurement Standards, Industrial Technology Research Institute, Hsin-Chu, Taiwan | [5]Institute for Solar Energy Research Hamelin, Emmerthal, Germany | [6]TUBITAK National Metrology Institute, Kocaeli, Turkey | [7]Laboratoire national de métrologie et d'essais, Paris cedex 15, France | [8]National Physical Laboratory, Teddington, Middlesex, UK

Correspondence: Afsaneh Eghbali (afsaneh.eghbali@aalto.fi)

Received: 1 December 2024 | **Revised:** 24 February 2025 | **Accepted:** 13 March 2025

Funding: EMPIR, Grant/Award Number: 19ENG01

Keywords: amorphous silicon | indoor photovoltaics | intercomparison | organic solar cells | short-circuit current | spectral responsivity

ABSTRACT

This study presents results of an intercomparison of indoor photovoltaics (PVs) among seven metrological institutes. Three types of solar cells were measured; organic and amorphous silicon cells representing current indoor products in the market and a reference solar cell. Three different light sources—AM1.5G, International Commission of Illumination Standard Illuminant A, and light-emitting diodes (LED) L41—were used at illuminance levels 100–2000 lx. Each laboratory reported short-circuit current as mandatory. Open-circuit voltage, maximum power, and differential spectral responsivity were reported where possible. Measurements revealed notable discrepancies. At the 1000 lx level, best agreement of 7% as standard deviation was achieved for the amorphous silicon cell using Standard Illuminant A. Similarly, the worst agreement of 37% was found for the reference cell using AM1.5G. Measurement methods varied across the laboratories. Some participants used lamps for Standard Illuminant A and LED L41. These measurements were generally in agreement but deviated from measurements with LED-based solar simulators, due to differences in measurement geometry, spectral properties, and treatment of infrared. Different illuminance measurement approaches, using either calibrated reference cells or luxmeters, further impacted consistency. This study highlights need for harmonized procedures to support reliable performance assessment of indoor PVs and gives recommendations to account for in standards.

1 | Introduction

Indoor solar cells are becoming increasingly important in the realm of the Internet of Things (IoT) [1, 2]. Indoor-photovoltaic (PV) systems can harvest energy from artificial light sources, such as light-emitting diodes (LEDs) or fluorescent lighting, ensuring continuous operation of IoT devices. Advancements in PV materials tailored for low-light environments, such as perovskites and organic PV, have improved energy conversion efficiencies indoors [3].

Indoor-PV devices allow for powering low-energy applications such as smart sensors, wearables, and IoT devices, where traditional batteries may not be practical or sustainable. By reducing reliance on disposable batteries, they help mitigate battery waste, contributing to environmental

sustainability and reducing the ecological impact of electronic devices.

While crystalline silicon (c-Si) dominates the PV market for outdoor applications, its performance under indoor lighting conditions is limited. The spectral mismatch between indoor-light sources and c-Si's spectral responsivity (SR), combined with its susceptibility to shunt losses at low light intensities, hinders its ability to achieve high efficiencies indoors. This has driven the development of alternative technologies, such as organic PVs, and perovskite solar cells that are specifically tailored for indoor environments [4].

Diversity in artificial light sources, such as LED, fluorescent, and incandescent lighting, each with different spectral distributions, makes it difficult to accurately characterize and compare indoor-PV devices [5, 6]. Even light sources manufactured by the same company, with identical nominal spectra, can show slight variations in their actual spectral outputs. The standard test conditions (STC) [7] for measuring PV cells outdoor are not relevant for indoor-ambient measurements because, typically, the artificial light sources do not have spectra similar to AM1.5 [8]. Indoor lighting is designed based on the human photopic response. The indoor-irradiance levels are typically much smaller than the defined 1000 W/m^2 for outdoors and specified as illuminance in [lx] rather than irradiance.

Efforts have been made to reach a universal guideline to accurately measure and report current–voltage (I–V) characteristics of indoor cells. Normalized spectra of five light sources, adopted for indoor-PV measurements, from the International Commission of Illumination (CIE), were proposed in the SEMI PV80-0218 [9] standard. The recent IEC TS 62607-7-2 [10] suggests using CIE FL10 [10], CIE LED B4 [11], or a user-defined light source. Even if consensus is reached among the community for one specific spectrum for indoor-PV measurements, it is challenging to achieve a spectrum in laboratory conditions with a specified irradiance or illuminance level. Hence, discrepancies among laboratories arise [12]. Indoor-PV measurements are typically reported for 1000 lx of illuminance or lower, which is the typical illuminance range of indoor environments. Studies show that using commercial luxmeters can end up in severe discrepancies among laboratories [13]. Inaccurate readings of commercial luxmeters often occur because they have been calibrated with a light source different from the one used for the indoor-PV measurements during their production. Also, if the angular dependence of the luxmeter deviates from $\cos(\theta)$, the luxmeter will inaccurately weight radiance from different angles, introducing an error [14]. In the case of diffuse illumination, which is the usual case of indoor lighting, this error can be significant. Some proposals have been made to reduce the discrepancies among laboratories because of the challenges mentioned earlier. National Institute of Standards and Technology (NIST) recommends using a method based on reference solar cells [15]. It has also been recommended to use a calibrated spectrometer instead of a luxmeter and convert the irradiance to illuminance mathematically [13].

The aforementioned procedures can be challenging, and measurement protocols need to be evaluated to achieve accurate and consistent measurements of indoor-PV devices. This article presents the results of an intercomparison activity of three indoor-PV cells, measured with three different light sources, among seven metrological institutes. Each laboratory carried out the measurements using their own procedures, with only the conditions for the measurement being set. The aim of the intercomparison activity was to evaluate the laboratory inter-comparability of the measurements, to identify common challenges and sources of errors, and to determine if the measurement setups used by the participants are consistent with each other. A special feature of the intercomparison is that the participants come from the solar PVs calibration community with their typical equipment based on solar simulators and reference solar cells, and from the photometry community with their typical equipment based on calibration light sources, photometers, and luxmeters. The findings and challenges identified in this intercomparison highlight need for changes to the current indoor standards, to improve the accuracy and consistency of indoor-PV measurements, promoting greater international alignment in the field.

2 | Comparison Artifacts and Measurands

One organic indoor cell, one amorphous silicon cell, and one world PV scale standard (WPVS) Si reference cell were used for the intercomparison. All laboratories measured the same set of cells. Table 1 introduces these artifacts, and Figure 1 presents their SRs. Of the cells used, organic and amorphous silicon cells represent current products available in the market

TABLE 1 | Solar cells measured in the intercomparison.

Solar cell type	Brand	Size	Remarks
Organic indoor cell	Epishine	5 × 5 cm^2	Mini-module, 6 cells, V_{oc} = 3.8 V
Amorphous silicon cell	Panasonic	4.85 × 5.83 cm^2	Mini-module, 8 cells, V_{oc} = 4.9 V
Reference cell	Allreal3a	2 × 2 cm^2	Silicon, V_{oc} = 0.65 V

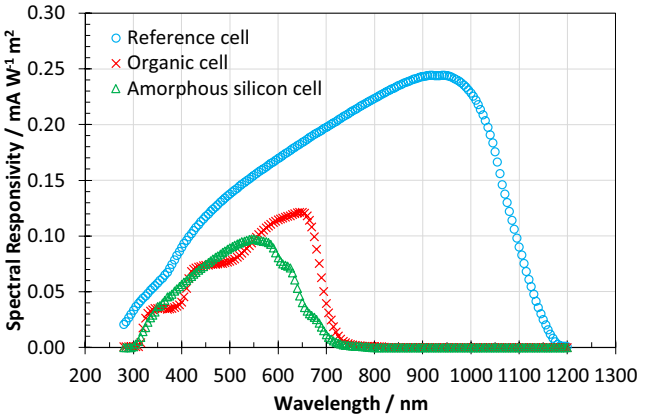

FIGURE 1 | Spectral responsivities of the solar cells of the comparison. Blue circles denote values for the reference cell, red crosses for the Epishine organic indoor solar cell, and green triangles for the Panasonic amorphous silicon cell. Measurements have been carried out by Laboratory 2 for 2000 lx illuminance of AM1.5G spectrum, and temperature of 25°C.

for indoor use. The reference cell was included as its behavior is well known, and most laboratories use these for the traceability of their setups.

Each laboratory had its own measurement setups and procedures. All cells within each laboratory were measured with the same laboratory procedures. All cells were equipped with a Lemo connector for four-wire measurements. The organic cell (Epishine) was flexible and semitransparent. For the organic cell and amorphous silicon cell, laboratories used their own vacuum chucks to mount them in their setups. The organic and amorphous silicon devices used in this study were technically mini-modules; however, for simplicity, they are referred to as "cells" throughout this article.

The measurands and requirements of the intercomparison are summarized in Table 2. Short-circuit current (I_{sc}) was a mandatory measurand that all participants in the intercomparison reported. Open-circuit voltage (V_{oc}), maximum power produced (P_{max}), and differential SR (DSR) were optional measurands. Measurement setups for DSR vary among participants, for spectral power responsivity and spectral irradiance responsivity, so two different units were accepted, the difference being related to the area of the cell. Results were normalized for comparison.

Measurements were realized with illumination under three light sources, CIE Standard Illuminant A [16], AM1.5G [8], and CIE LED B3 [11], also known as CIE reference spectrum L41 [17]. Figure 2 presents the normalized spectra of the light sources used in the intercomparison. Of the sources specified, CIE LED B3 represents typical lighting used in indoor applications. Incandescent lamps are rarely used anymore, but CIE Standard Illuminant A was included because it is still the dominant light source used in calibration of luxmeters. AM1.5G is applicable for indoor use in places with large windows. It was also included because of its wide use in outdoor applications and its well standardized properties.

Laboratories either measured the cells with the defined light sources or converted their results mathematically using DSR method. Results were reported at illuminance levels (E_v) of 100, 500, 1000, 1500, and 2000 lx. All calculations were to be carried out over the wavelength range of 280–1200 nm. Not all labs measured the samples at all possible conditions, depending on their available light sources and system specifications. The project protocol did not define a specific angular distribution, because availability of light sources differs. Some laboratories are familiar with using solar simulators, whereas others carried out calibrations using lamps.

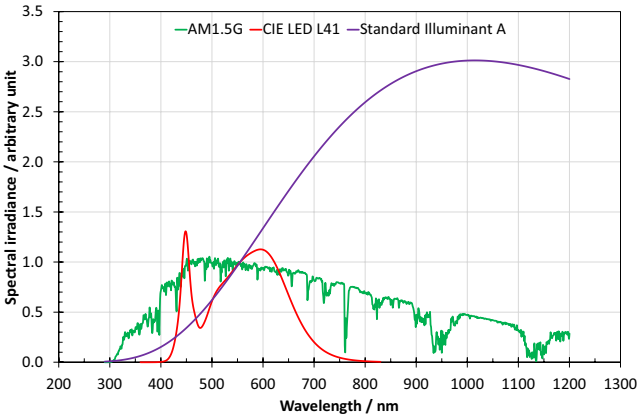

FIGURE 2 | Normalized spectral irradiances of the three light sources used in the intercomparison. Purple, green, and red lines denote Standard Illuminant A, AM1.5G, and CIE LED L41 spectra, respectively.

The measurement conditions selected in this intercomparison deviate from the existing indoor standard [18], because this intercomparison was shaped and started before the final version of the standard and its publication. However, the specific conditions will not impact the findings such as challenges associated with indoor measurements.

3 | Participants and Their Measurement Procedures

Measurements of the round robin took place during January–December 2023. Participants in the round robin are listed in Table 3. One of the laboratories was selected as the pilot laboratory, coordinating the logistics of the intercomparison and analyzing the results. It also acted as the reference laboratory measuring all cells in the beginning and at the end of the round robin. Another laboratory was selected as a secondary reference, measuring cells directly after the pilot. The measurements were expected to be challenging, as this is the first intercomparison for indoor-PV devices, hence, the provision of a secondary reference.

The intercomparison had a round robin structure, partners received the samples from the previous laboratory and shipped them to the next one. All participants sent their measurement results to the pilot after all partners had finished their measurements. Since the pilot also measured the samples, it sent its results to the secondary reference laboratory before other participants sent their results to the pilot.

TABLE 2 | Measurands, units, and requirements for the photovoltaics in the intercomparison.

Measurand	Unit	Light source	E_v [lx]	Necessity for intercomparison	Uncertainty budget
I_{sc}	A	Standard Illuminant A, AM1.5G, LED L41	100, 500, 1000, 1500, 2000	Mandatory	Recommended
V_{oc}	V			Optional	Recommended
P_{max}	W			Optional	Recommended
DSR	A W^{-1} or mA W^{-1} m^2			Optional	Recommended

TABLE 3 | Participants of the intercomparison.

Institution	Country
Aalto University	Finland
Laboratoire National de Metrologie et d'Essays (LNE)	France
Institut für Solarenergieforschung in Hameln (ISFH)	Germany
Physikalisch-Technische Bundesanstalt (PTB)	Germany
Industrial Technology Research Institute Incorporated (ITRI)	Taiwan
Scientific and Technological Research Council of Turkey (TUBITAK)	Turkey
National Physical Laboratory (NPL)	UK

The participants had different traceability chains and measurement procedures that are defined in Sections 3.1–3.7. Table 4 presents a summary of the details of the measurement procedures. Results in this paper are handled anonymously, and the order of the laboratories in Table 3 has been shuffled in the results.

3.1 | Participant 1—Pilot

3.1.1 | DSR Measurements

The indoor cells were measured for DSR using a setup similar to that described in [19]. Halogen lamps were used to provide bias light for the cells, with the light level controlled by adjusting the number of lamps and the lamp current. The bias light was set so that the reference cell produced a DC current of ~1.32 mA, equivalent to what it would generate under AM1.5G conditions at an illuminance of 1000 lx. The setup included 30 temperature-stabilized LEDs, driven by pulsed current, to measure DSR. The weak-modulated LED signal generated an induced photocurrent in the solar cell, which was detected using a lock-in amplifier (Stanford Research Systems SR830). A Keithley 2420 source meter was employed to maintain a negligible voltage across the cells. A reference cell (119–2016), traceable to Physikalisch-Technische Bundesanstalt (PTB), was measured before and after each cell. Since the cells were not temperature-stabilized, their temperature increased to 26°C during the measurements, while the laboratory temperature was 24°C.

3.1.2 | *I–V* Sweeping

A solar simulator with AM1.5G was not available; hence, *I–V* measurements were only carried out for Standard Illuminant A and L41. I_{sc} values for AM1.5G were derived mathematically at varying illuminance levels from DSR measurements. The light sources were mounted, one at a time, on an optical bench. The illuminance was adjusted by varying the distance between the cell and the light source. An illuminance meter was used to set illuminances during measurements. Later in the data analysis, illuminance levels were corrected using signals measured with a reference cell, traceable to PTB, because it had lower uncertainty than the luxmeter. The solar cells were then installed at the distances from the sources determined by illuminance. The illuminance level was measured at the beginning and end of each measurement of the cells. A Keithley 2420 source-meter was used for measuring the *I–V* curves of the solar cells. Since the cell temperatures were not stabilized, they reached ~26°C during the measurements. Temperatures, currents, and voltages under Standard Illuminant A and L41 were corrected with method 4 of IEC 60891:2021 [20].

3.2 | Participant 2—Secondary Reference

3.2.1 | DSR Measurements

Participant 2 used its DSR facility for the measurements. Monochromatic irradiance was produced using either a xenon lamp or a halogen lamp in conjunction with a monochromator system, followed by imaging optics to create uniform illumination of the device under test (DUT). The DUT was simultaneously illuminated with white bias light generating bias irradiance levels from 0 to 100 W/m^2. The temperature of the DUT was stabilized to 25°C ± 0.2 K. The absolute DSR of the DUT was measured at different bias irradiance levels to determine the nonlinearity of the DSR. The SR as well as the I_{sc} were then derived mathematically from the DSR measurements using the different tabulated indoor reference spectra as reference spectral irradiance and the derived irradiance values calculated from the reference illuminance levels. The reference detector was a calibrated photodiode traceable to International System of Units (SI) via the cryogenic radiometer at PTB. For indoor-PV devices, prior to measurements, the impact of the chopping frequency on the DSR was investigated. If no significant effect was observed, measurements were made with a chopping frequency of 78 Hz. Otherwise, a chopping frequency of 5 Hz was applied.

3.2.2 | *I–V* Sweeping

The *I–V* measurements were performed on an *I–V* facility consisting of a 4-quadrant current–voltage source and a precision reference shunt resistance with a rated value of 0.1 Ω. The irradiance was adjusted in such a way that the I_{sc} obtained was the same as the I_{sc} derived from the earlier calibration of the differential spectral irradiance responsivity. With the aid of the *I–V* characteristics measuring system, different voltages were applied to the cell. The resulting current was measured as a voltage drop across the calibrated shunt resistance. Synchronously, the voltage *V* was recorded at the contacts *V*+ and *V*– of the reference solar cell, and the time-dependent stability of the irradiance was recorded via a monitor solar cell for correction.

3.3 | Participant 3

3.3.1 | DSR Measurements

For SR measurements, a LOANA system from PV tools was employed. This system utilizes the DSR approach as described in reference [21]. Bias light was provided by halogen lamps, with neutral density filters used to attenuate their irradiance to the desired levels as low as 100 lx.

TABLE 4 | Details of the measurement procedures of participants.

Participant 1			
	AM1.5G	**CIE LED L41**	**CIE Standard Illuminant A**
Type of light source used	DSR measured, I_{sc} calculated by DSR	LED lamp (LISA) manufactured by PTB	Osram Wi41/G photometric standard lamp
Measurement mode and time	CW, >1 h	CW, ~15 min	CW, ~20 min
Wavelength region for calculations	280–1200 nm (Illuminance calculation 360–830 nm)	360–830 nm	280–1200 nm (illuminance 360–830 nm)
Angular distribution/geometry	DSR measured with point sources (LED) at distance of ~80 cm	Diameter of LED source ~3 cm at distances between 442 mm (2000 lx)–1845 mm (100 lx).	Point source (2×2 cm^2) at distances between 661 mm (2000 lx)–3038 mm (100 lx).
Nonuniformity	1% for 5×5 cm^2, 0.6% for 2×2 cm^2	<1%	<1%
Method for adjusting illuminance	Mathematical	Distance	Distance
Spectral mismatch correction [%]	–	–	–
Device for measuring Illuminance	–	Luxmeter (later verified with PTB reference cell)	
Model	–	Gigahertz-Optik X1+VL-3701	
Traceability	–	PTB (both luxmeter and reference cell)	
Uncertainty	–	3% for luxmeter, <1% for reference cell	
Input geometry	–	Luxmeter cosine corrected, $f_2 \leq 1.5\%$, reference cell unknown	
Participant 2			
Type of light source used	DSR measured, I_{sc} calculated using DSR		
Measurement mode and time	CW, 1 day	CW, 1 day	CW, 1 day
Wavelength region for calculations	280–1200 nm (Illuminance calculation 360–830 nm)	360–830 nm	280–1200 nm (illuminance 360–830 nm)
Angular distribution/geometry	Divergent beam with an aperture angle between the marginal rays of maximally 1°		
Nonuniformity	<1%	<1%	<1%
Method for adjusting illuminance	Mathematical	Mathematical	Mathematical
Spectral mismatch correction [%]	–	–	–
Device for measuring illuminance	–	–	–
Participant 3			
Type of light source used	LED solar simulator		
Measurement mode and time	CW	CW	CW
Wavelength region for calculations	350–1100 nm	350–1100 nm	350–1100 nm
Angular distribution/geometry	13×13 cm^2 light engine at a distance of 33.5 cm from the sample plane		
Nonuniformity	<2%	<2%	<2%
Method for adjusting illuminance	Neutral density filters on sample, LED channel levels are adjusted to reproduce the target spectrum		
Spectral mismatch correction [%]	–	–	–
Device for measuring illuminance	Luxmeter		
Model	MAVOLUX 5032C/B USB		
Traceability	PTB		
Uncertainty	1.5%		
Input geometry	Cosine corrected luxmeter head		

TABLE 4 | (Continued)

Participant 4			
Type of light source used	LED solar simulator	LED B lamp Osram	Osram FEL photometric lamp
Measurement mode and time	CW, >1 h	CW, ~15 min	CW, >~40 min
Wavelength region for calculations	360–1100 nm	380–780 nm	Unlimited, so up IR
Angular distribution/geometry	LED-based lighting source, distance to cell 66 cm (2000 lx) –148 cm (500 lx).	LED lamp, distance to cell 18–52 cm (100–1000 lx)	Point source (10×2 cm^2) at distances 68 cm (2000lx)–296.5 cm (100 lx).
Nonuniformity	<1%, 3×3 cm^2	<1%, 3×3 cm^2	<1%, 3×3 cm^2
Method for adjusting illuminance	Distance	Distance	Distance
Spectral mismatch correction [%]	Amorphous-Si: 0.985	Amorphous-Si: 0.906	Amorphous-Si: 0.997
	Organic cell: 1.014	Organic cell: 0.972	Organic cell: 1.002
	Reference cell: 1.030	Reference cell: 0.998	Reference cell: 1.002
Device for measuring illuminance	Photometer	Photometer	Luxmeter Head
Model	PRC Krochmann	PRC Krochmann	PRC Krochmann
Traceability	TÜBİTAK	TÜBİTAK	TÜBİTAK
Uncertainty	0.8%	0.8%	$U = 1.5\%$, $f' < 1.5$
Participant 5			
Type of light source used	LED solar simulator	Custom LED simulator, diffuser plate lit by LEDs	Custom indoor lighting simulator, diffuser plate lit by incandescent lamps, IR region filtered away with low pass filter cutting at 780 nm
Measurement mode and time	CW, >1 h	CW, >1 h	CW, >1 h
Wavelength region for calculations	300–780 nm	300–780 nm	300–780 nm
Angular distribution/geometry	30×30 cm^2 light engine at a distance of 50 cm from the sample plane		
Nonuniformity	<1% for 16×16 cm^2; <2% for 19×19 cm	<2% for 20×20 cm^2	<2% for 20×20 cm^2
Method for adjusting illuminance	ND filters used in simulator	Adjusted by simulator electronics	Adjusted by simulator electronics
Spectral mismatch correction [%]	–	–	–
Device for measuring Illuminance	Luxmeter		
Model	HIOKI FT3424		
Traceability	NIST		
Uncertainty	1.2%		
Input geometry	Class AA meet CIE ISO/CIE 19476 and CIE 063 and CIE023 and JIS C 1609–1 and DIN 5032		
Participant 6			
Type of light source used	–	20 cm diameter LED light source fitted with a diffuser for homogeneous output beam	12′ diameter integrating sphere with 50 mm diameter output beam, fitted with a tungsten–halogen lamp at CCT = 2856 K
Measurement mode and time	–	CW	CW
Wavelength region for calculations	–	380–780 nm (Luxmeter)	380–780 nm (Luxmeter)
Angular distribution/geometry	–	Source is placed 1 m from the PV cell	Source placed 500 mm from the cell
Uniformity	–	0.5%, 100 mm × 100 mm at module position	1%, 100 mm × 100 mm at module position
Method for adjusting illuminance	–	Variation of the feeding current of the thermally stabilized LEDs	Variable size aperture in front of the lamp to vary the output illuminance

(Continues)

TABLE 4 | (Continued)

Participant 6			
Spectral mismatch correction [%]	–	0.5%	0.1%
Device for measuring Illuminance	–	Luxmeter	
Model		LMT PMH-120	
Traceability		LNE	
Uncertainty		2%	
Input geometry		Cosine corrected	
Participant 7			
Type of light source used	–	Cree CXA2 5000 K CRI 70 white LED	–
Measurement mode and time	–	CW, ~30 min	–
Wavelength region for calculations	–	380–780 nm	–
Angular distribution/geometry	–	Semi-collimated with an estimated angular diversion of 9.3°	–
Nonuniformity	–	2%, 6×6 cm^2	–
Method for adjusting illuminance	–	Spatial dithering using a digital micromirror device	–
Spectral mismatch correction [%]	–	Amorphous-Si: (1.044 ± 0.042) Organic cell: (0.994 ± 0.016) Reference cell: (0.973 ± 0.014)	–
Device for measuring illuminance	–	Reference Cell Rera KG5 Si Traceable via third-party calibration to NIST	–

[a)]Abbreviations: CW = Continuous wave, NIST = National Institute of Standards and Technology, CCT = Correlated Colour Temperature.

3.3.2 | *I–V* Sweeping

The *I–V* measurements were also conducted using the LOANA system from PV tools. The light source for these measurements was a Wavelabs Sinus 70 LED solar simulator with 21 channels generating light between 350 nm and 1100 nm wavelengths. The required spectral irradiances (AM1.5G, LED L41, and Standard Illuminant A) were approximated by adjusting the LED channels. Neutral density filters were used to reduce the total irradiance to desired levels ranging from 100 to 2000 lx. These filters were placed directly on the front surface of the solar cells.

3.4 | Participant 4

3.4.1 | DSR Measurements

The DSR setup consisted of a double monochromator, a tungsten lamp, output optics, a biased light source, and detection electronics. A monochromatic light beam was generated from the exit slit of a single monochromator and directed onto the surfaces of the reference and the test PV devices, ensuring homogeneous illumination. Additionally, the PV devices were biased using a xenon light source. The monochromator light was chopped, and the current generated by the DUTs was measured using a lock-in amplifier. The SRs of the indoor-PV devices were determined by taking the ratio of the currents from the DUTs and reference devices and then multiplied by the reference irradiance values. Measurements were made in the wavelength range of 300–1100 nm. Cell temperatures were not controlled during the measurements.

3.4.2 | *I–V* Sweeping

The *I–V* characteristics of the indoor-PV devices were measured on an optical bench. The setup included a lamp holder, optical bench, and a detection unit, with Illuminant A and LED L41 light sources mounted on a lamp holder. The reference luxmeter and the PV devices were placed on a translation stage, which moved along the optical bench to achieve desired illuminance levels and horizontally to measure illuminance. A Keithley source-meter (2410) was used to measure the *I–V* curves. Measurements were made by first adjusting the illuminance levels, then preconditioning the devices to stabilize them, and determining suitable voltage step lengths and sweep times. Forward and reverse *I–V* scans were performed, and the steady-state conditions of I_{sc} and V_{oc} were monitored. Consistent measurements were obtained and repeated three times to assess repeatability. Cell temperatures were monitored using a Fluke multimeter. For AM1.5G spectrum, WaveLabs LS-2000 LED solar simulator was used as the light source.

3.5 | Participant 5

3.5.1 | DSR Measurements

The system included a xenon light source, a monochromator, and a lock-in amplifier. Temperature control was managed using thermoelectric cooling and heating with Peltier elements or resistive heaters. Halogen lamps provided the bias light, while

Si and Ge detectors, along with a reference cell traceable to PTB, were used for measurements. Irradiance levels were adjusted based on the SR of the reference cell.

3.5.2 | *I–V* Sweeping

Measurements with CIE Standard Illuminant A were carried out using a custom indoor-lighting simulator that accommodates multiple CIE standard illuminants: D65 (6500 K, North American daylight), TL84 (4100 K, European shop fluorescent), CWF (4150 K, cool white fluorescent), U30 (3000 K, shop lighting), and A (2856 K, typical home lighting). For Standard Illuminant A, a specific lamp was used to produce the light. Light above 780 nm was filtered away with a low pass filter. The simulator allowed for adjustable light intensities from dark to 2500 lx, with a nonuniformity of <2% and temporal instability of <2%, in accordance with SEMI PV80 [9, 22]. For AM1.5G conditions, a WaveLabs SINUS-300 LED solar simulator with an ND filter for low lux levels was used. LEDs above 780 nm were not used. For LED L41, a custom LED simulator with adjustable spectrum and intensity was employed.

During *I–V* measurements in both dark and illuminated conditions, the RTOS *I–V* Method [22] (also known as the asymptotic or dynamic *I–V* Method) was employed for optimal repeatability. Measurements were performed with forward and backward scan directions, maintaining a stable sample temperature of 25°C with less than 0.5°C fluctuation. Irradiance and illuminance were measured using a NIST-traceable spectroradiometer (StellarNet) and a national metrology laboratory (NML)-traceable luxmeter.

3.6 | Participant 6

3.6.1 | *I–V* Sweeping

The measurement setup included two light sources: an L41 LED, custom-built by the laboratory, and a variable-luminance integrating-sphere-based incandescent source. The LED source was temperature-controlled to ensure a stable spectral distribution. The illuminance level at the PV device reference plane was measured using a luxmeter and was adjusted between 50 Lx and 2000 Lx by varying either the source-to-device distance or the power supply current of the source. The *I–V* curve was recorded in both forward and backward directions using an IET LABS PRS-200 programable variable resistor, which also supports measurements of I_{sc} and V_{oc}. Voltage readings were obtained with a KEITHLEY 2000 voltmeter, while current was measured using a Stanford Research Systems SR570 current amplifier in conjunction with the same voltmeter.

3.7 | Participant 7

3.7.1 | DSR Measurements

Due to the lack of commercial reference cells available for indoor-PV testing, a WPVS packaged KG5 silicon reference cell was calibrated at illumination levels below 500 lx, against a calibrated reference photodiode, and the photodiode was calibrated by a third party against a reference traceable to NIST primary standards. The *SR* system consisted of a xenon light source, a Bentham TC300 monochromator, a lock-in amplifier Stanford Research Systems SR830, temperature control, and available bias light. Based on the reference cell's *SR* and the photopic response curve, the expected generated current at the specific lux levels was calculated, so that it could be used to set the correct irradiance levels at the sample plane. *SR* measurements of all

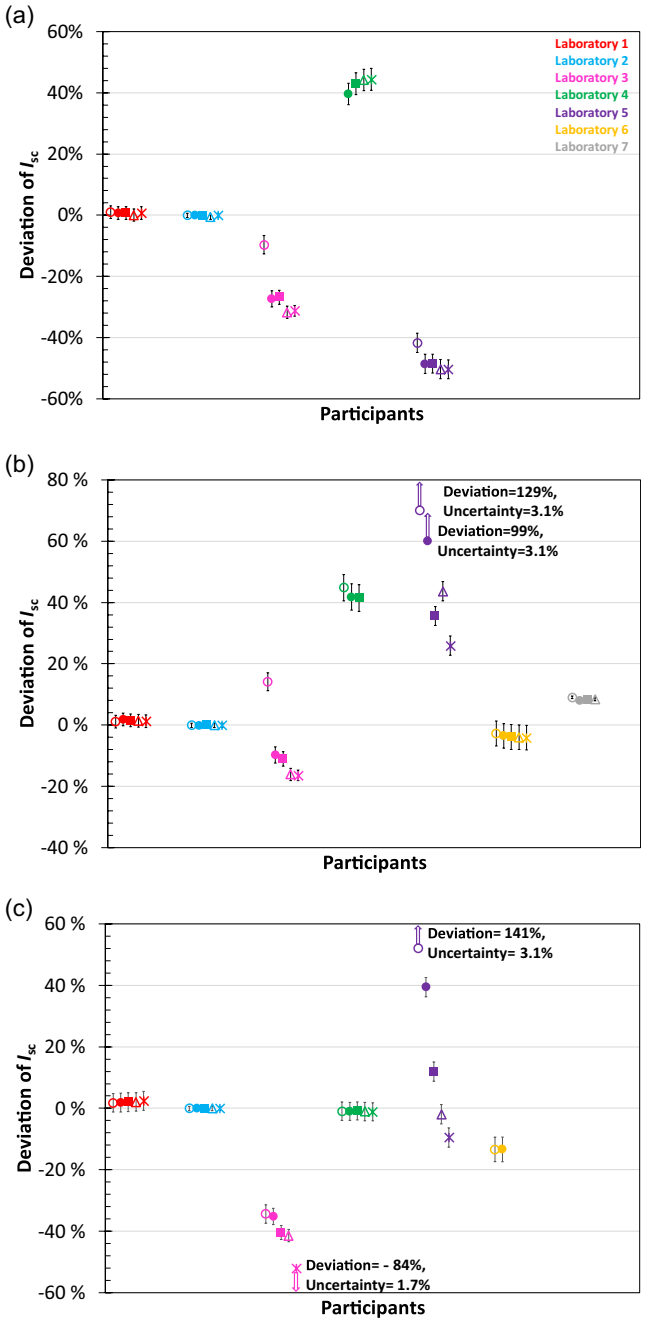

FIGURE 3 | Deviations of I_{sc} from the reference values for the reference cell, measured under three different irradiance conditions of (a) AM1.5G, (b) LED L41, and (c) Standard Illuminant A. The symbols represent different illuminance levels, with empty circles for 100 Lx, filled circles for 500 Lx, squares for 1000 Lx, triangles for 1500 Lx, and crosses for 2000 Lx. The color coding of laboratories is given in figure legend. The error bars denote expanded uncertainties of comparison at the level of $k = 2$.

indoor-PV samples were acquired with 2000 lx biasing with white LEDs. Spectral mismatches were applied to set the effective irradiance at the required light levels for each sample.

3.7.2 | Indoor-PV System

A new indoor-PV testing system [23] for indoor-PV performance measurements compliant with IEC TS 62607-7-2 [10] was used. The system is based on a digital micromirror device (DMD) coupled with an LED light source (Cree CXA2 5000 K, CRI 70 white LED). The system delivers a pseudo collimated beam at the sample plane. The use of the DMD enables to reduce the illuminance level at the sample plane by controlling the number of pixels turned 'on' as opposed to controlling the current through the LED. As the reflectivity of the DMD micromirrors is uniform across the visible spectrum, the spectrum of the projected light source will not change when the pattern changes. Methods of using optical attenuation to reduce the light intensity have been reported, but spectral deviations were also observed.

The beam goes through three baffles to reduce stray light toward the sample, then a flat front coated mirror at a 45° angle guides the beam to the sample plane so samples can be placed horizontally on the measurement platform. The platform is placed on top of an x–y stage to enable measurements of spatial nonuniformities within the region of interest. A Keithley 2401 source meter is used for I–V measurements. The sample platform includes temperature control and feedback, with additional temperature control of the enclosure space, to keep both the sample platform and the enclosure space at 25°C. The spectrum of the simulator was selected considering IEC TS 62607-7-2 [10] to be as close as possible to CIE LED B4. Deviation of the spectrum from the reference was corrected mathematically. Spectral mismatch was lower than 5%. Measurements were corrected to the LED L41 spectrum for meaningful comparisons.

4 | Data Analysis

The first and last measurements carried out by the pilot revealed that none of the cells changed significantly. I_{sc} measurements at the start and end of the intercomparison showed changes of 0.02%, 0.67%, and 0.03% for the reference cell, organic cell, and the amorphous silicon cell, respectively. Considering the uncertainty of measurements, the cells did not change during the intercomparison.

All seven participants in the intercomparison measured and reported I_{sc} of the solar cells, as this was a mandatory parameter. Most participants also specified combined standard uncertainties u or expanded uncertainties U for their values. The V_{oc} and P_{max} of the cells were reported by majority of the participants. They are presented in the appendix of this paper. Laboratory 4 provided two sets of data, with spectral mismatch (SMM) corrections applied to the latter. Only the corrected results are presented in this article. The DSRs of the cells reported are presented in Sections 5.1–5.3.

Due to the large deviations noted, it was difficult to assign reference values for the quantities. Results of participants i that were in agreement were selected and their weighted average

$$I_{sc,ref} = \frac{\sum_{i=1}^{n} \frac{I_{sc,i}}{u_{I_{sc,i}}^2}}{\sum_{i=1}^{n} \frac{1}{u_{I_{sc,i}}^2}} \quad (1)$$

where n is the number of selected laboratories, was used as the reference. The uncertainty of the reference value, when the measurands $I_{sc,i}$ have uncertainty of $u_{I_{sc,i}}$ and a weight of $\frac{1}{u_{I_{sc,i}}^2}$, was calculated as [24]

TABLE 5 | Reference values for the measurands of the intercomparison and standard deviations (STDEV) of all measuring laboratories for the reference cell.

AM1.5G											
E_v	lx	100	–	500	–	1000	–	1500	–	2000	–
I_{sc}	A	0.00013	23	0.00064	36	0.0013	37	0.0019	39	0.0026	39
V_{oc}	V	0.25	10	0.35	6.7	0.40	5.4	0.42	5.5	0.44	5.5
P_{max}	W	0.000014	39	0.00012	54	0.00030	53	0.00049	56	0.00069	55
CIE LED L41											
E_v	lx	100	–	500	–	1000	–	1500	–	2000	–
I_{sc}	A	0.000050	37	0.00025	32	0.00050	18	0.00075	19	0.0010	15
V_{oc}	V	0.17	11	0.29	6.2	0.33	3.0	0.36	3.3	0.38	2.2
P_{max}	W	0.0000032	62	0.000035	45	0.000089	22	0.00015	24	0.00022	18
Standard Illuminant A											
E_v	lx	100	–	500	–	1000	–	1500	–	2000	–
I_{sc}	A	0.00039	54	0.0019	25	0.0039	21	0.0058	20	0.0078	45
V_{oc}	V	0.32	8.2	0.42	4.0	0.47	4.6	0.49	3.6	0.51	10
P_{max}	W	0.000065	71	0.00050	29	0.0011	24	0.0019	23	0.0026	49

$$u_{I_{sc,ref}} = \frac{1}{\sum_{i=1}^{n} \frac{1}{u_{I_{sc,i}}^2}} \sqrt{\sum_{i=1}^{n} \left(\frac{1}{u_{I_{sc,i}}^2} u_{I_{sc,i}} \right)^2} = \frac{1}{\sqrt{\sum_{i=1}^{n} \frac{1}{u_{I_{sc,i}}^2}}} \quad (2)$$

In most cases, only Laboratories 1 and 2 were in agreement, so the reference value and its uncertainty were calculated using data of two laboratories.

For all participants j, deviations from the reference value were calculated as

$$\Delta I_{sc,j} = \frac{I_{sc,j}}{I_{sc,ref}} - 1 \quad (3)$$

The standard uncertainty of this deviation was calculated as

$$u_{\Delta I_{sc,i}} = \sqrt{u_{I_{sc,j}}^2 + u_{I_{sc,ref}}^2} \quad (4)$$

where $u_{I_{sc,j}}$ is the uncertainty reported by each participant. For laboratories providing uncertainties, the results were also analyzed by comparing the deviations with their associated expanded uncertainties U ($\Delta I_{sc,j}$), using

$$E_n = \frac{\Delta I_{sc,j}}{U(\Delta I_{sc,j})} \quad (5)$$

as a criterion [25]. In a successful comparison, $|E_n|$ should be below 1.

5 | Results

5.1 | Si Reference Cell

Figure 3 shows comparison results for the short-circuit currents of the reference cell. Missing data points indicate that the laboratory did not report those values. The data points marked with an arrow instead of an error bar fall outside the representative data range; therefore, their deviations and uncertainties are indicated next to each symbol.

Laboratories 1 and 2 are in agreement within uncertainties for all three light sources. Other laboratories have deviations in at least one light source. The agreement of laboratories can be explained to large extent by similarities in the measurement methods. For AM1.5G, both laboratories used the DSR method and calculated the I_{sc} values with same traceability and nearly collimated geometry. For LED L41 and CIE Standard Illuminant A, Laboratory 2 used DSR method. Laboratory 1 used standard light sources.

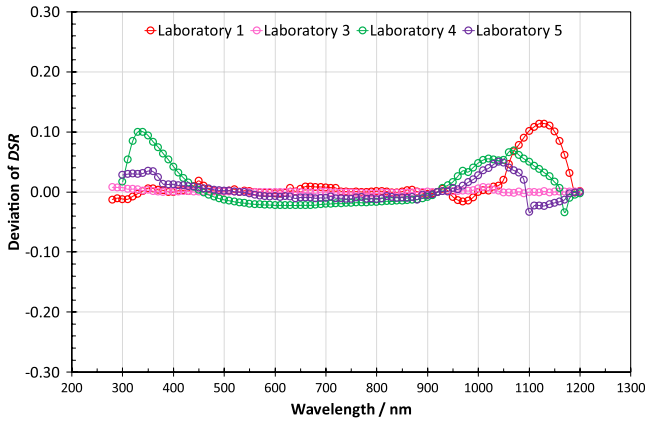

FIGURE 4 | Deviations of participants in DSR measurements of the reference cell from the reference laboratory. All DSR results are normalized to the maximum value of the reference laboratory at the wavelength of 920 nm shown in Figure 1.

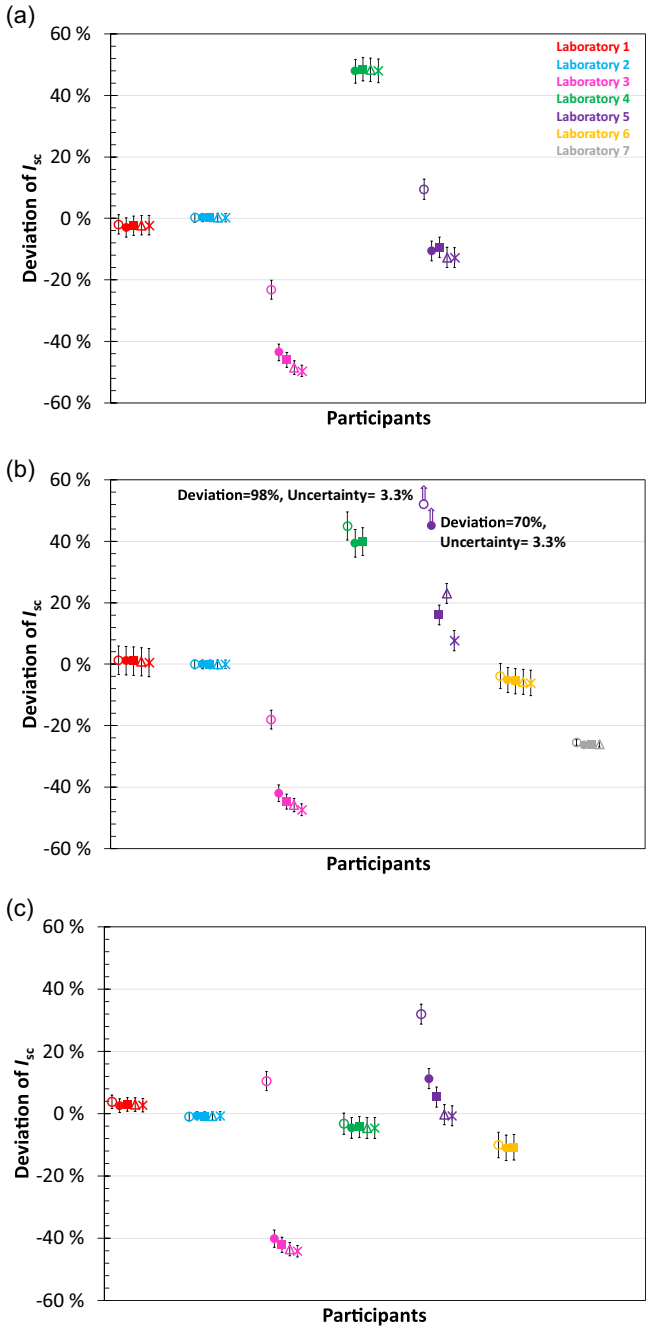

FIGURE 5 | Deviations of I_{sc} from the reference values for the organic cell, measured under three different irradiance conditions of (a) AM1.5 G, (b) LED L41, and (c) Standard Illuminant A. The symbols are the same as those in Figure 3.

Although being different in method, they both use nearly collimated light and same traceability.

With AM1.5G, Laboratory 3 consistently reported lower results, measuring approximately 29% below the reference value on average across all measurements, with a smaller deviation for illuminance of 100 lx. With CIE LED L41, Laboratory 3 had best agreement, 14% higher than reference for 100 lx illuminance and ~13% lower for higher illuminances. With Standard Illuminant A, results were ~47% below the reference value on average across all measurements. Measurements were carried out by attenuating light with neutral density filters. The deviation has correlation with the infrared (IR) content of the source being highest with CIE Standard Illuminant A producing most IR, and smallest with LED L41 that has no IR.

With Standard Illuminant A, Laboratory 4 had good agreement within uncertainties. In this measurement, they employed Standard Illuminant A lamp instead of a solar simulator. With AM1.5G and CIE LED L41, Laboratory 4 measured ~43% higher than reference. Both deviating measurements were made with LED sources. Geometries differed as AM1.5G was realized using a simulator with extended size, and L41 was a lamp with smaller size. The results thus suggest an issue with measuring LEDs instead of an issue with geometry.

Results of Laboratory 5 have a strong dependence on illuminance level for both CIE LED L41 and Standard Illuminant A. Results start with deviations of the order of 100% at low lux levels and approach reference values at higher illuminance levels. Varying the intensity was obtained with electronics of the simulator. Obviously, this method changes the intensity or the spectrum in an unpredictable way. For AM1.5G there was a constant deviation of −48%. Here, varying the level was obtained using neutral density filters. This produces more repeatable results, but there is a deviation in a similar way to Laboratory 3 also using filters. Laboratory 5 cut all light sources for light above 780 nm to be consistent with SEMI PV80, which other laboratories did not do. This could explain 41% of the 48% deviation noted with AM1.5G.

Laboratory 6 has an agreement within uncertainties with LED L41, where their deviation of −3.6% fits just within uncertainties. For Standard Illuminant A, there is a deviation with $E_n = -3.3$.

Laboratory 7 only measured with CIE LED L41. The results deviate with $E_n = 17$, due to small uncertainties estimated.

Results for V_{oc} and P_{max} were very similar to the I_{sc} results. Therefore, they are presented in the appendix. Table 5 presents reference values and standard deviations of all measurands I_{sc}, V_{oc}, and P_{max} that the laboratories reported for the three light sources measuring the reference cell.

Five laboratories reported DSR of the reference cell. Figure 4 presents the deviations of the DSR measurements of Laboratories 1, 3, 4, and 5 relative to Laboratory 2 that was chosen as the reference. The DSR measurements are used to correct for spectral mismatch. Thus, the DSR data of all participants were normalized to the maximum value of 1 at 920 nm, which is the wavelength of maximum DSR as determined by Laboratory 2. The deviations from the reference laboratory were then calculated by subtraction on the scale of normalized responsivity. This method of analysis shows deviations smaller in the regions where responsivity is low, as compared to comparing relative deviations, thus showing the effect that the deviations have.

The DSR data reveal that all laboratories are in quite good agreement. Laboratory 1 deviates in the region 1050–1200 nm, indicating problems in IR measurements. Laboratory 4 deviates slightly

TABLE 6 | Reference values for the measurands of the intercomparison and standard deviations (STDEV) of all measuring laboratories for the organic cell.

AM1.5G											
E_v	lx	100	–	500	–	1000	–	1500	–	2000	–
I_{sc}	A	0.000038	14	0.00019	33	0.00038	34	0.00057	36	0.00076	36
V_{oc}	V	3.5	1.3	3.9	1.3	4.0	1.0	4.1	1.2	4.2	1.2
P_{max}	W	0.000074	22	0.00054	39	0.0011	38	0.0016	39	0.0022	38
CIE LED L41											
E_v	lx	100	–	500	–	1000	–	1500	–	2000	–
I_{sc}	A	0.000030	34	0.00015	33	0.00030	25	0.00045	24	0.00060	24
V_{oc}	V	3.4	2.5	3.8	1.8	4.0	1.1	4.1	1.1	4.1	1.3
P_{max}	W	0.000060	44	0.00040	36	0.00086	25	0.0013	23	0.0017	22
Standard Illuminant A											
E_v	lx	100	–	500	–	1000	–	1500	–	2000	–
I_{sc}	A	0.000042	14	0.00021	19	0.00042	19	0.00062	21	0.00083	22
V_{oc}	V	3.5	1.2	3.9	0.75	4.0	1.0	4.1	2.0	4.2	2.5
P_{max}	W	0.00011	20	0.00059	17	0.0011	16	0.0018	18	0.0024	18

in 300–400 and 900–1200 nm regions. In the regions where deviations are observed, the signal is relatively low, as seen in Figure 1, which explains the higher deviations.

5.2 | Organic Cell

Figure 5 presents comparison results for the short-circuit currents for the organic indoor cell.

Results with the organic cell have similar trends with the Si reference cell measurements, but also differences.

Laboratories 1 and 2 are in agreement with each other within their uncertainties for all three light sources in the intercomparison, although this time the agreement is not that good for the Standard Illuminant A. The reasons for agreement are the same as earlier.

Laboratory 3 measured ~45% lower than reference for all light sources with smaller deviations at low illuminance levels at 100 lx. What is noteworthy is that now the deviations are practically the same for all light sources. The organic cell has very low responsivity in the IR region which could explain the difference from the noted behavior with reference cell that has high responsivity in IR.

Again, Laboratory 4 was close to reference values for Standard Illuminant A with $E_n = -1.3$, as it employed a Standard Illuminant A lamp. With the AM1.5G, Laboratory 4 measured ~48% higher than the reference, and ~41% higher with LED L41. Also here, the results indicate problem in measuring LED-based sources, independent of geometry.

Deviations of Laboratory 5 show again dependence on illuminance levels, but to lesser extent than with the reference cell. The deviations from the reference values are also a factor of 2 smaller. Results approach the reference values with increasing illuminance with Standard Illuminant A. With AM1.5G, results have smaller deviations than LED L41, especially for the lower lux levels. The difference in behavior from the reference cell could be explained by the missing IR responsivity of the organic cell.

Laboratory 6 deviates slightly with both the Standard Illuminant A and LED L41, with $E_n = -2.0$ and $E_n = -1.3$, respectively.

Laboratory 7 only measured using LED L41, and the results were constantly ~26% lower than the reference.

Since the organic cell was semitransparent and not covered on the back side, deviations were expected due to differences in

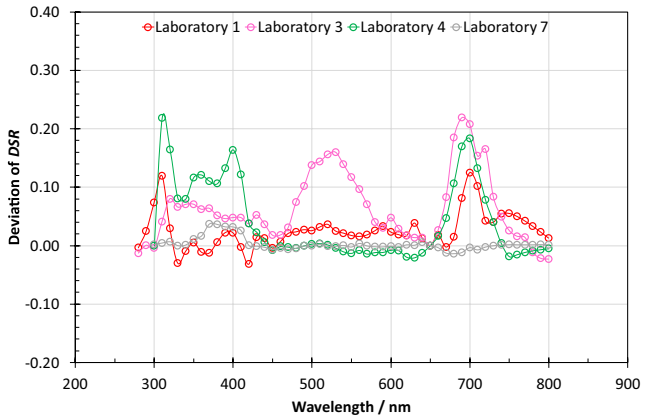

FIGURE 6 | Deviations of participants in DSR measurements of the organic cell from the reference laboratory. All DSR results are normalized to the maximum value of the reference laboratory at the wavelength of 650 nm shown in Figure 1.

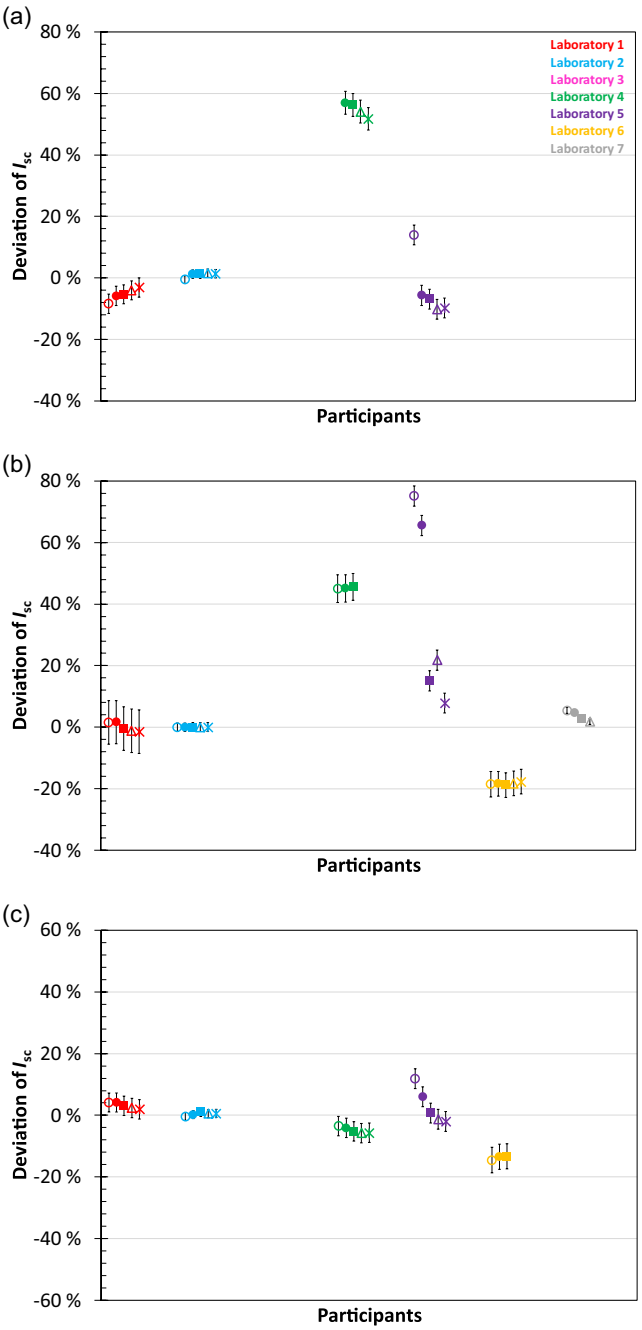

FIGURE 7 | Deviations of I_{sc} from the reference values for the amorphous silicon cell, measured under three different irradiance conditions of (a) AM1.5 G, (b) LED L41, and (c) Standard Illuminant A. The symbols are the same as those in Figure 3.

the reflectivity of the black platform used by different participants, and since it was technically a mini-module, any nonuniformities in its structure could impact its performance.

Table 6 presents standard deviations of all measurands I_{sc}, V_{oc}, and P_{max} that the laboratories reported for the three light sources measuring the organic cell. Results are similar to those for the reference cells.

Figure 6 presents the deviations of DSR measurements of Laboratories 1, 3, 4, and 7 relative to Laboratory 2 for the organic cell. The DSR data were normalized to 1 at 650 nm, which was the peak wavelength reported by Laboratory 2. Deviations from the reference laboratory were then calculated by subtraction on the normalized scale. The responsivity is very small at wavelengths larger than 800 nm. It is noteworthy that this sample was a mini-module where nonuniformities may cause issues. The participants measured the sample in an over-illuminated mode under uniform illumination to prevent effects of nonuniformity.

The DSR data in Figure 6 reveal that Laboratory 7 has good agreement within the entire wavelength region. Laboratory 1 is generally in agreement with the reference, but measures high at the extremes, where responsivity drops, which could arise from large bandwidth used. Laboratories 3 and 4 also measure high near 700 nm. Laboratory 4 originally showed systematic wavelength-dependent deviation especially within the range 300–500 nm, which appeared to be due to mistakenly reporting external quantum efficiencies as DSR.

5.3 | Amorphous Silicon Cell

Figure 7 presents a comparison of short-circuit current measurements for the amorphous silicon cell across different laboratories.

For the AM1.5G light source, the reference value was determined as the weighted average of measurements from Laboratories 1, 2, and 5, as they are in agreement. For the CIE LED L41 light source, the reference value was based on the weighted average of measurements from Laboratories 1 and 2, as these two were in close agreement, while other laboratories showed notable deviations. For the Standard Illuminant A light source, the reference value was obtained as the average of all laboratories, with their associated weights, since they showed good agreement with one another.

Laboratories 1 and 2 are in best agreement with each other for LED L41, and their largest deviation of ~6% is for AM1.5G.

Laboratory 3 did not measure amorphous silicon cell, due to size restrictions in their setup.

Laboratory 4 measured 54% and 45% higher than the reference under AM1.5G and LED L41, respectively. It deviates slightly for Standard Illuminant A by $E_n = -1.4$. Result is similar to other cells confirming problems in measuring LED-based sources.

Laboratory 5 has its largest deviations for LED L41, especially for lower illuminance levels. Their results approach the reference values for Standard Illuminant A and lower illuminances of AM1.5G. The responsivity of amorphous silicon cell is limited to wavelengths below 700 nm. Good agreement with these measurements further confirms the conclusion that deviations of Laboratory 5 with the other two cells are related with the missing IR radiation of the sources.

Laboratory 6 deviates for Standard Illuminant A and L41 by $E_n = -3.3$ and -4.6, respectively.

Laboratory 7 only measured for LED L41 and had smaller deviations at larger illuminance values with $E_n = 2.4$.

TABLE 7 | Reference values for the measurands of the intercomparison and standard deviations (STDEV) of all measuring laboratories for the amorphous silicon cell.

AM1.5G											
E_v	lx	100	–	500	–	1000	–	1500	–	2000	–
I_{sc}	A	0.000032	11	0.00015	30	0.00031	27	0.00045	27	0.00060	26
V_{oc}	V	4.8	2.5	5.6	3.3	5.8	2.7	5.9	2.4	6.0	2.7
P_{max}	W	0.000067	35	0.00053	26	0.0011	22	0.0015	20	0.0017	18
CIE LED L41											
E_v	lx	100	–	500	–	1000	–	1500	–	2000	–
I_{sc}	A	0.000025	30	0.00012	27	0.00024	20	0.00036	14	0.00048	11
V_{oc}	V	4.7	6.3	5.4	5.1	5.6	6.1	5.6	4.2	5.6	5.0
P_{max}	W	0.000056	41	0.00038	25	0.00081	18	0.0012	13	0.0014	11
Standard Illuminant A											
E_v	lx	100	–	500	–	1000	–	1500	–	2000	–
I_{sc}	A	0.000027	10	0.00013	7.9	0.00027	6.8	0.00040	3.5	0.00052	3.4
V_{oc}	V	4.8	1.4	5.5	3.6	5.7	3.4	5.8	4.5	5.9	4.7
P_{max}	W	0.000080	18	0.00042	6.4	0.00090	11	0.0013	11	0.0015	8.4

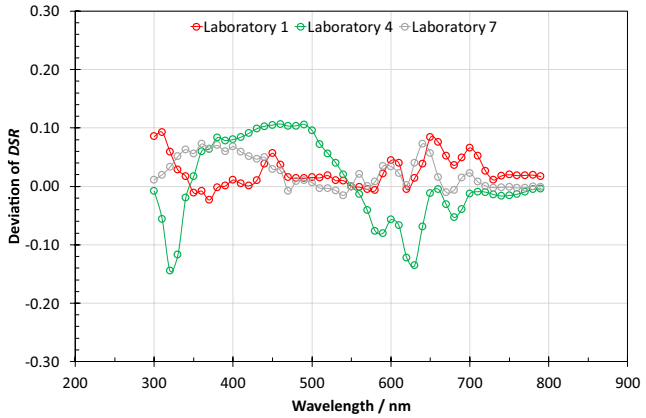

FIGURE 8 | Deviations of participants in DSR measurements of the amorphous silicon cell from the reference laboratory. All DSR results are normalized to the maximum value of the reference laboratory at the wavelength of 550 nm shown in Figure 1.

Any nonuniformities in the structure of this mini-module could impact its performance.

Table 7 presents standard deviations of all laboratories reporting measurands I_{sc}, V_{oc}, and P_{max} for three light sources used in the intercomparison. What is noteworthy is the good agreement of results for Standard Illuminant A. The standard deviation of I_{sc} ranges from 3.4% to 10%, when it was of the order of 20% with the organic cell and ranged from 20% to 54% with the reference cell. This could indicate problems of measuring or setting the illuminance level of the simulators. The SR of the amorphous silicon cell is relatively close to the $V(\lambda)$ [26] curve, i.e., the SR of a luxmeter used to set the illuminance level. With this detector–light source combination, the mismatch corrections are smallest, and the measurement conditions are close to those used in the calibration of the luxmeter. Amorphous silicon also does not respond to IR light, so deviations in setting or measuring the spectral irradiances in the IR region do not affect the measurements.

Figure 8 presents the deviations of the DSR measurements of Laboratories 1, 4, and 7 relative to Laboratory 2 for the amorphous silicon cell. The DSR data were normalized to 1 at 550 nm, which was the peak wavelength reported by Laboratory 2. Deviations from the reference laboratory were then calculated by subtraction on the normalized scale. Figure 8 is plotted for the wavelength region where the cell has responsivity. To prevent issues with nonuniformity, the participants measured this mini-module in an over-illuminated mode under uniform illumination.

The DSR data reveal that Laboratories 1 and 7 are in agreement with the reference, although they exhibit some deviations probably due to interpolation. Laboratory 4 shows some spectral deviations throughout the entire region.

6 | Discussion

The comparison revealed significant discrepancies among participants.

Short-circuit currents showed the best agreement with the amorphous silicon cell under the Standard Illuminant A light source. Also, other measurands were more consistent with this combination. SR of the amorphous silicon cell is significantly closer to SR of a luxmeter than the responsivity of the reference cell. This combination is thus very close to the calibration conditions of luxmeters that are still calibrated with Standard Illuminant A light sources in National Metrology Institutes and calibration laboratories.

Calibrated luxmeters provide the most accurate illuminance measurements for spectra close to the light source used in calibration due to their imperfect adaptation to $V(\lambda)$. For other sources, spectral mismatch correction is needed. Under illumination of Standard Illuminant A, the standard deviation of I_{sc} ranged from 3.4% to 10% for the amorphous silicon cell, approximately 20% for the organic cell, and from 20% to 54% for the reference cell.

The Si reference cell showed the highest deviations compared to all cells, which may be attributed to the cell's high responsivity in the IR region. Luxmeters used as reference do not measure at all in the IR region which the PV device can still detect. To compensate for this effect, a second spectral mismatch correction is necessary. This requires accurate *SR* measurements and precise spectral irradiance measurements, particularly in the IR region.

Some commercial luxmeters experience a zero-offset issue. The electronics detect negative readings when measuring dark but the internal software of the display shows these as zero. This phenomenon could explain discrepancies at the lowest illuminance levels observed with Laboratory 3.

Participants had quite good agreement in DSR measurements with the best agreement for the reference cell and the poorest for the organic cell. This is quite as expected, because reference cells are well defined and stable from metrological point of view, and laboratories have long experience in calibrating them for DSR. Measurement setups also utilize similar reference cells for their traceability, so it is natural that results agree better, the closer the responsivities of reference cell and DUT are. The organic cell was semitransparent so differences in the reflectivity of the background may change responsivity. With semitransparent devices, nonreflective background for measuring should be used and standardized. The organic PV was a relatively large mini module and laminated instead of protected with glass. Thus, nonuniformities of irradiance at the sample plane or diffuse radiation may have affected measurements.

Two types of light sources were used by participants for measurements: lamps on optical rails and LED-based solar simulators. Laboratory 2 also used DSR to calculate short-circuit currents for all sources, and Laboratory 1 used this approach for AM1.5G. The calibrations based on lamps and DSR were generally in better agreement than results with simulators. There are several possible reasons for this.

With lamps, illuminance levels may be changed by varying the distance. This does not change the lamp spectrum, and illuminance can be measured reliably. Solar simulators were attenuated with neutral density filters, which caused discrepancies especially with sources containing IR, or with the control

electronics, which caused illuminance-dependent behavior in the measurements. With these methods, it turns out to be essential to measure the spectral irradiance with a calibrated spectroradiometer in the measurement plane for each single illuminance level, since the relative spectral irradiance, and hence the spectral mismatch correction, might change significantly.

Standard SEMI PV80 on calibrating indoor solar cells defines light sources to be used in indoor cell calibrations. These include, e.g., Standard Illuminant A, D65, U30, CWF, and TL84, but only up to 780 nm wavelength, although the sources would extend into IR. Lamps and most of the simulators used in the comparison extended into IR, but spectra of some simulators were cut at 780 nm to be consistent with the standard. This caused deviations of the order of 40%. Since indoor-PV applications most likely will include silicon solar cells due to their low cost and commercial availability, the definitions of the indoor light sources should include the full spectral range of silicon, i.e., 300–1200 nm. Only if the reference spectra are defined in the full spectral range of all possible indoor-PV technologies, spectral mismatch corrections can be properly applied. Although LED lighting is already the dominant and definitely the future technology, halogen lamps and discharge lamps are still in use and should not a priori be excluded as an application for indoor-PV metrology and standardization, especially when photometric traceability is still based on Standard Illuminant A.

The project protocol did not define measurement geometry. Although the effect of measurement geometry could not directly be seen in the results, its inclusion would improve harmonization in comparisons. Geometry of simulators differs significantly from geometry obtained with lamps due to the larger, extended size of simulators, compared to the near-point source nature of lamps. Luxmeters are generally cosine-corrected, but angular responsivities of solar cells may deviate from cosine, especially at larger angles [27].

Laboratories 1, 2, and 7 used reference cells for measuring illuminances. Other participants used calibrated luxmeters. Traceability of illuminance measurements varied. Three laboratories were traceable to PTB, two to NIST, one to LNE, and one to Tübitak. No differences due to traceability could be noticed due to other larger discrepancies. Luxmeters used were of high quality and low uncertainties. Good spectral matching to the luminous efficiency function is essential, otherwise spectral-mismatch corrections for the correct determination of the illuminance level are needed. Even with perfect matching, SR of a luxmeter differs significantly from that of most PVs leading to large additional spectral mismatch corrections when the calibration light source differs significantly from the reference conditions, i.e., contains spectral content outside the visible range. Results suggest that one participant may have had measurement issues with LED sources possibly originating from illuminance measurements.

For successful comparisons, it is essential to get reliable reference values. In this sense, standard lamps appear to be preferable to LED-based solar simulators. For setting illuminance, it is beneficial to verify luxmeter readings with a reference cell, that was calibrated to the reference illuminance conditions, or to use the reference cell with known or measured irradiance to derive illuminance. Reference cells bear the advantage over luxmeters, that they can be spectrally matched to the indoor-PV devices by suitable optical filters, thereby minimizing spectral mismatch errors. Also, the angular response is usually more similar to indoor-PV devices compared to luxmeters, so that angular effects might cancel out. Another approach to achieving reproducible reference values is to derive I_{sc} of an indoor-PV device from DSR and then perform subsequent I–V measurements using the DSR-derived currents as a self-reference. However, this significantly increases the calibration effort, thus preventing its use for regular testing of indoor-PV products.

For varying illuminance levels, changing distance has advantages over other methods such as neutral density filters or tuning the power of the light source, provided that uniformity can be verified. The latter might introduce changes in the spectrum and hence lead to illuminance-dependent spectral mismatch corrections. In all cases, the nonuniformity of the light field might change. It is advised to measure the spectral irradiance in the respective measurement plane for each illuminance.

Compared to standard PV testing at high irradiance levels, residual room light has only a minor impact on measurement results, so usually no background subtraction due to ambient light is applied. For indoor PV, this is different. There, a dark measurement subtraction of the straylight coming from the room should be mandatory.

Indoor-PV devices are still in the early stages of development, and the current standards for indoor-PV measurements is not yet fully optimized, which has led to significant discrepancies in comparative studies among laboratories. Nevertheless, these comparisons represent a crucial step toward improving standardization in the field. With continued efforts, laboratories are expected to achieve better comparability in their measurements, leading to more reliable progress in indoor-PV technologies.

Acknowledgments

The results reported in this article are derived from activities within the frame of the EMPIR project 19ENG01 Metro-PV (Metrology for emerging PV applications) that has received funding from the EMPIR program cofinanced by the Participating States and the European Union's Horizon 2020 research and innovation program. This work is also part of the Research Council of Finland Flagship Programme, Photonics Research and Innovation (PREIN), decision number 346529, Aalto University. NPL authors acknowledge funding by the Department for Science, Innovation & Technology (UK) through the National Measurement System, and the International Science Partnerships Fund (ISPF) project "Setting the Standards for Semiconductors".

Data Availability Statement

The data that support the findings of this study are available from the corresponding author upon reasonable request.

References

1. X. Liu, S. Xu, B. Tang, and X. Song, "Indoor Organic Photovoltaics for Low-Power Internet of Things Devices: Recent Advances, Challenges, and Prospects," *Chemical Engineering Journal* 497 (2024): 154944.

2. X. Zhu, J. Xu, H. Cen, Z. Wu, H. Dong, and J. Xi, "Perspectives for the Conversion of Perovskite Indoor Photovoltaics into IoT Reality," *Nanoscale* 15, no. 11 (2023): 5167–5180.

3. D. Müller, E. Jiang, P. Rivas-Lazaro, et al., "Indoor Photovoltaics for the Internet-of-Things – A Comparison of State-of-the-Art Devices from Different Photovoltaic Technologies," *ACS Applied Energy Materials* 6, no. 20 (2023): 10404–10414, https://doi.org/10.1021/acsaem.3c01274.

4. S. Biswas and H. Kim, "Solar Cells for Indoor Applications: Progress and Development," *Polymers* 12, no. 6 (1338): 2020.

5. M. Freunek, M. Freunek, and L. M. Reindl, "Maximum Efficiencies of Indoor Photovoltaic Devices," *IEEE Journal of Photovoltaics* 3, no. 1 (2012): 59–64.

6. S. Kim, M. Jahandar, J. H. Jeong, and D. C. Lim, "Recent Progress in Solar Cell Technology for Low-Light Indoor Applications," *Current Alternative Energy* 3, no. 1 (2019): 3–17.

7. IEC 60904-4: 2019, *Photovoltaic Devices - Part 4: Photovoltaic Reference Devices - Procedures for Establishing Calibration Traceability*.

8. IEC 60904-3: 2018, *Photovoltaic Devices-Part 3: Measurement Principles for Terrestrial Photovoltaic (PV) Solar Devices with Reference Spectral Irradiance Data*.

9. SEMI PV80-0218: 2018, *Specification of Indoor Lighting Simulator Requirements for Emerging Photovoltaic and Perovskite Solar Cell (PSC)*.

10. IEC TS 62607-7-2: 2023, *Nanomanufacturing - Key Control Characteristics - Part 7-2: Nano-Enabled Photovoltaics - Device Evaluation Method for Indoor Light*.

11. CIE 015: 2018, *Colorimetry, 4th Edition*.

12. B. H. Hamadani, "2.11-Accurate Characterization of Indoor Photovoltaic Performance," *Journal of Physics: Materials* 6 (2023): 10–1088.

13. Y. Cui, L. Hong, T. Zhang, et al., "Accurate Photovoltaic Measurement of Organic Cells for Indoor Applications," *Joule* 5, no. 5 (2021): 1016–1023, https://doi.org/10.1016/j.joule.2021.03.029.

14. J. M. Jailani, A. Luu, E. Salvosa, et al., "*Accurate Performance Characterization, Reporting, and Benchmarking for Indoor Photovoltaics*, arXiv:2408.13485, 2024.

15. B. H. Hamadani and M. B. Campanelli, "Photovoltaic Characterization under Artificial Low Irradiance Conditions Using Reference Solar Cells," *IEEE Journal of Photovoltaics* 10, no. 4 (2020): 1119–1125.

16. ISO/CIE 11664-2: 2022(en), *Colorimetry—Part 2: CIE Standard Illuminants*.

17. CIE 2023, *CIE Reference Spectrum L41*. International Commission on Illumination (CIE).

18. IEC TS 62607-7-2: 2023, *Nanomanufacturing – Key Control Characteristics – Part 7-2: Nano-Enabled Photovoltaics – Device Evaluation Method for Indoor Light*.

19. P. Kärhä, H. Baumgartner, J. Askola, et al., "Measurement Setup for Differential Spectral Responsivity of Solar Cells," *Optical Review* 27, no. 2 (2020): 195–204, https://doi.org/10.1007/s10043-020-00584-x.

20. IEC 60891: 2021, *Photovoltaic Devices - Procedures for Temperature and Irradiance Corrections to Measured I-V Characteristics*.

21. J. Metzdorf, "Calibration of Solar Cells. 1: The Differential Spectral Responsivity Method," *Applied Optics* 26, no. 9 (1987): 1701–1708, https://doi.org/10.1364/AO.26.001701.

22. Y.-S. Long, S.-T. Hsu, and T.-C. Wu, "Induction of Internal Capacitance Effect in Performance Measurement of OPV (organic Photovoltaic) Device by RTOSM (real-Time One-Sweep Method," *Journal of Energy and Power Engineering* 8, no. 6, 2014.

23. D. E. Parsons, G. Koutsourakis, and J. C. Blakesley, "Performance Measurements for Indoor Photovoltaic Devices: Classification of a Novel Light Source," *APL Energy* 2, no. 1 (2024): 016110.

24. P. R. Bevington and D. K. Robinson, *Data Reduction and Error Analysis for the Physical Sciences* (3ed., McGraw-Hill, 2003).

25. SFS-EN ISO/IEC 17043 : 2023:en*General requirements for the competence of proficiency testing providers*.

26. T. 1 CIE 018 : 2019, *CIE Spectral Luminous Efficiency for Photopic Vision*.

27. F. Plag, I. Kröger, T. Fey, F. Witt, and S. Winter, "Angular-Dependent Spectral Responsivity—Traceable Measurements on Optical Losses in PV Devices," *Progress in Photovoltaics: Research and Applications* 26, no. 8 (2018): 565–578.

Supporting Information

Additional supporting information can be found online in the Supporting Information section.